Enabling Multi-Hop Concurrent Transmissions in 60 GHz Wireless Personal Area Networks

Jian Qiao, Lin X. Cai, Xuemin (Sherman) Shen, *Fellow, IEEE,* and Jon W. Mark, *Life Fellow, IEEE*

Abstract—Millimeter-wave (mmWave) communications is a promising enabling technology for high rate (Giga-bit) multimedia applications. However, because of the high propagation loss at 60 GHz band, mmWave signal power degrades significantly over distance. Therefore, a traffic flow being transmitted over multiple short hops can attain higher throughput than that over a single long hop. In this paper, we first design a hop selection metric for the piconet controller (PNC) to select appropriate relay hops for a traffic flow, aiming to improve the flow throughput and balance the traffic loads across the network. We then propose a multi-hop concurrent transmission (MHCT) scheme to exploit the spatial capacity of mmWave WPANs by allowing nodes to transmit concurrently in communication links without causing harmful interference. The analysis of concurrent transmission probability and time division multiplexing demonstrates that the MHCT scheme is capable of improving the time slot utilization. Extensive simulations are conducted to validate the analytical results and demonstrate that the proposed MHCT scheme can improve the average traffic flow throughput and network throughput.

Index Terms—Multi-hop, concurrent transmission scheduling, millimeter Wave WPANs, resource utilization.

I. INTRODUCTION

COMMUNICATIONS at 60 GHz band is referred to as millimeter-wave (mmWave) communications because the wavelength at this band is in the order of millimeters. Over the past decade, the wireless communication community has become increasingly interested in the worldwide 60 GHz radio frequency band [1], [2], [5]–[7]. In 2001, the Federal Communications Commission (FCC) approved an unprecedented 7 GHz spectrum between 57 and 64 GHz for commercial use, which enables multi-Gbps wireless connections for bandwidth-intensive multimedia applications related to consumer electronics, such as uncompressed video streaming and kiosk high speed downloading service. With the recent advances of Radio Frequency Integrated Circuits (RFIC) design in mmWave band [9], [10], [16], there have been growing interests in standardizing and drafting specifications for mmWave systems to fulfill the multi-Gbps requirement by standardization bodies, including the IEEE 802.15.3c [11] and IEEE 802.11 VHT [12] task groups.

One fundamental distinguishing feature of mmWave communications is the high propagation loss. As the free space propagation loss increases proportionally as the square of the carrier frequency, the propagation loss at mmWave band is much higher than that at lower frequency bands, e.g., 28 dB

higher than at 2.4 GHz. The path loss becomes more serious since oxygen absorption peaks at 60 GHz. A directional antenna with high directivity gain can be utilized to combat the severe path loss to achieve high data rate in mmWave communications, and to allow more efficient spatial reuse. Since non-line-of-sight (NLOS) transmissions in 60 GHz channels suffer from significant attenuation and a shortage of multipath [4], [25], mmWave WPANs rely on line-of-sight (LOS) propagation to achieve high data rate. In case moving obstacles block the LOS propagation between the source and the destination, relaying can be used for data transmission.

As mmWave signals attenuate significantly over distance, it is beneficial to employ relaying to transmit the signal from the source to the destination to reduce signal loss due to attenuation. In this paper, we design a novel hop selection metric for the piconet controller (PNC) to choose proper relaying nodes to forward data, aiming to improve the flow throughput and achieve load-balancing across the network. To further improve the network performance, we propose a multi-hop concurrent transmission (MHCT) scheme to allow concurrent transmissions for non-interfering communication links over the mmWave channel. By properly breaking one long-hop (i.e., low rate) transmission into multiple short-hop (i.e., high rate) transmissions and allowing non-interfering nodes to transmit concurrently, the network resources can be efficiently utilized to improve flow throughput and network throughput.

The main contributions of this paper are four-fold. First, we design a novel metric to select relays to forward data. Second, we propose a concurrent transmission scheduling algorithm to exploit the spatial reuse in mmWave WPANs, considering the unique features of mmWave communications, e.g., link outage and directional antenna. Third, it is demonstrated that the MHCT scheme can increase the opportunities for channel reuse and improve time division multiplexing in comparison to single hop concurrent transmission (SHCT) scheme. Finally, extensive simulations are conducted to demonstrate that the proposed scheme is effective and efficient.

The remainder of the paper is organized as follows. The system model is described in Section II. The MHCT scheme with a hop selection metric is proposed in Section III. The performance of the proposed scheme is analyzed in Section IV and evaluated by intensive simulations in Section V. Related works are presented in Section VI, followed by concluding remarks in Section VII.

II. SYSTEM MODEL

We consider an indoor WPAN composed of multiple wireless nodes (WNs) and a single PNC. All nodes are equipped with an electronically steerable directional antenna and are

able to direct their beams towards each other for transmission and reception. With the accurate localization service provided by the mmWave indoor system [14], [15], the PNC can obtain the network topology information for transmission scheduling which is in time division multiplexing mode in mmWave WPANs. Moving obstacles in the room may block the LOS link between the source and the destination, causing transmission data rate degradation. The proposed MHCT scheme relies on LOS link for data transmission in each hop.

A. mmWave Communication

The capacity of an additive white Gaussian noise (AWGN) channel with broadband interference assumed as Gaussian distribution is given by:

$$C = W \log_2[1 + \frac{P_R}{(N_0 + I)W}] \qquad (1)$$

where P_R is the received signal power, W is the system bandwidth, N_0 and I are the one-side power spectral densities of white Gaussian noise and broadband interference, respectively.

When the transmission rate is below channel capacity, the received signal power can be calculated using the Friis transmission equation and is given by

$$P_R(d) = P_T G_R G_T (\frac{\lambda}{4\pi})^2 (\frac{1}{d})^n \qquad (2)$$

where P_T is the transmitted power, G_T and G_R are respectively the antenna gains of the transmitter and receiver. λ is the wavelength, d is the transmission distance between the transmitter and the receiver, and n is the path loss exponent, which is normally determined using a measurement approach (usually in the range of 2 to 6 for indoor environment [25]). By combining (1) and (2), the data rate can be obtained as

$$R \le C = W \log_2[1 + \frac{P_T G_R G_T \lambda^2}{16\pi^2 (N_0 + I)W d^n}] \qquad (3)$$

The minimum hop-count metric which usually favors the hops with long distance, significantly reduces the received signal strength and degrades the achieved traffic flow throughput. According to (3), the flow throughput reduction over distance is more serious in mmWave communication due to its large bandwidth and small wavelength.

B. Antenna Model

We apply an ideal "flat-top" model for directional antenna [26]. Every node employs an antenna with B beams, each of which spans an angle of $2\pi/B$ radians. Each beam has a fixed beamwidth with none overlapping beam radians so that B beams can collectively maintain the seamless coverage of the entire plane. Directional antennas are characterized by their pattern functions that measure the power gain $G(\phi)$ over the angle ϕ. The normalized pattern function is defined as

$$g(\phi) = \frac{G(\phi)}{G_{max}} \qquad (4)$$

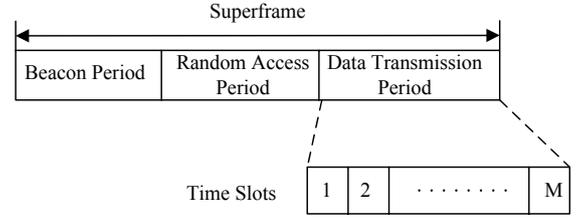where

$$G_{max} = max_\phi G(\phi) \qquad (5)$$

Fig. 1. IEEE 802.15.3 MAC structure.

In an ideal case, the antenna gain is constant, i.e., unit gain within the beamwidth and zero outside the beamwidth [27],

$$g(\phi) = \begin{cases} 1, & | \phi | \le \dfrac{\Delta\phi}{2} \\ 0, & \text{otherwise} \end{cases} \qquad (6)$$

where $\Delta\phi = 2\pi/B$ is the antenna beamwidth. In our system, the transmitter and receiver antenna gains are $G_T = G_R = 1$ within the antenna beamwidth, while $G_T = G_R = 0$ outside the beamwidth.

C. Directional MAC Structure

The MAC protocol is based on the IEEE 802.15.3 superframe structure, as shown in Fig. 1. A superframe consists of three periods: beacon, random access and data transmission. During the beacon period, the PNC activates all its beams and sends out beacon frames in all directions to the WNs for synchronization, scheduling information and other management information distribution. The scheduling information includes the transmission starting time, a maximum allowed transmission (TXOP) duration and antenna beam direction. The beacon period is followed by a random access period consisting of several mini-slots. An active WN chooses a mini-slot randomly to transmit its request to the PNC. The PNC schedules contention-free peer-to-peer transmissions in the data transmission period of the following superframe. When directional antenna is used for both transmission and reception, there is a so-called deafness problem when a directional receiver does not point its beamwidth towards the direction of the transmitter and thus fails to receive a message from the sender. To avoid the deafness problem caused by directional antenna, which involves very complicated MAC design [3], the PNC remains operating in the omni-directional mode by switching all its beams on during the random access period, and uses one beam for data transmission in the subsequent data transmission period. By operating in the omni-directional mode, the PNC can hear the transmissions from all the directions. To fully exploit the mmWave channel capacity, we improve the IEEE 802.15.3 MAC by allowing multiple nodes to transmit data concurrently. Concurrent transmission in two links is feasible if and only if any transmitter is outside the beamwidth of the other receiver or does not direct its beam to the other receiver if it is in the beamwidth of the other receiver [20], [30]. Our work focuses on transmission scheduling in the data transmission period.

III. MULTI-HOP CONCURRENT TRANSMISSION SCHEME

In this section, we first propose a hop selection metric to determine the multiple hops for a traffic flow to increase the

flow throughput and achieve load-balancing. Then a MHCT algorithm to improve the spatial reuse of mmWave WPANs is presented.

Fig. 2.　Illustration for hop selection.

A. Hop Selection Metric

To achieve high transmission data rate for each traffic flow, short links are usually preferred for hop selection. Therefore, more hops may be involved in the transmission of each flow, which results in heavy traffic loads in the network. In addition, if traffic aggregates at a node, congestion may occur and this node becomes a bottleneck for the network. Therefore, we need to select appropriate relay hops to improve the network throughput, considering both the link length and the traffic loads at the node.

When the PNC receives a transmission request, it determines the appropriate relaying hops based on the global network information, including the distance from one node to all its neighbors, antenna directions steering towards their neighbors, and the traffic load of each node. The traffic load of each node is defined as the number of transmissions running or to run at each node. More concurrent transmissions can be supported by well balancing the traffic loads in the network. To determine the relaying hops for a pair of transmitter and receiver, a weighted graph is generated by the PNC. The weight associated with link $(A \rightarrow B)$ between nodes A and B is given by

$$w(A, B) = \frac{d^n(A, B)}{E[d^n]} + \frac{F(B)}{E[F]} \tag{7}$$

where $d(A, B)$ is the length of link $(A \rightarrow B)$, $F(B)$ is the traffic load of node B, $E[d^n]$ is the average link length to the power n among all the links in the network currently, and $E[F]$ is the average node traffic load, which is defined as the summation of the traffic loads of all the nodes in the network divided by the number of nodes. We use normalized value for hop selection to smooth the large difference between the node's loads and link lengths. To improve flow throughput and achieve load balancing, the transmission rate and the node's load should jointly contribute to the hop selection. In (3), the transmission data rate is a function of d^n, which is included in the metric (7) to favor multi-hop high data rate transmissions. For example, as shown in Fig. 2, there are four options from the source to the destination, $S \rightarrow B \rightarrow C \rightarrow D$, $S \rightarrow B \rightarrow D$, $S \rightarrow C \rightarrow D$, and $S \rightarrow D$. According to the hop selection metric in (7), given $n = 2$ for example, the weights of the options are in the following sequence $W_{S \rightarrow D} > W_{S \rightarrow B \rightarrow D} = W_{S \rightarrow C \rightarrow D} > W_{S \rightarrow B \rightarrow C \rightarrow D}$ while $W_{S \rightarrow B \rightarrow C \rightarrow D} > W_{S \rightarrow C \rightarrow D} = W_{S \rightarrow B \rightarrow D} > W_{S \rightarrow D}$ if the item of d^n $(n \geq 2)$ in (7) is replaced by link length d. Due to the severe propagation loss at mmWave band, the option $S \rightarrow B \rightarrow C \rightarrow D$ is more likely to achieve higher flow throughput in comparison with the others. The hops with minimum summation weights from the source to the destination are chosen for the traffic flow to transmit data. The hops selected for each traffic flow heavily depend on the network topology, but the proposed metric provides important insights on hop selection in densely deployed mmWave WPANs: 1) the selected relay nodes should be close to or on the line between
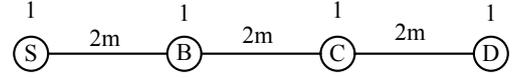
the source and the destination; 2) the accumulated weights achieve the minimum value if the lengths of selected hops for each flow are almost the same, based on the inequality of arithmetic and geometric means (AM-GM inequality); and 3) with a greater number of short hops for each traffic flow, the summation of link length to the power n for each flow decreases while the summation of node loads increases. This tradeoff bounds the number of hops for each flow.

B. The Proposed Concurrent Transmission Scheme

Based on the hop selection metric in the previous subsection, we propose an MHCT scheme as follows: initially, the PNC activates all the beams to collect network topology information and node's load information. The PNC maintains these information and updates it when there is any change. Multimedia applications in mmWave WPANs (i.e., uncompressed video streaming and kiosk high speed downloading) usually are long-lived flows and their statistical traffic demands do not change frequently. Without loss of generality, we consider the scenarios in which each node sends its traffic load information to the PNC every m superframes. When a transmission request is received, the PNC calculates $E[d^n]$ and $E[F]$ based on the traffic load and topology information received in the random access period, and then generates a weighted graph where the weight of each link is calculated according to (7). The PNC chooses the path with the lowest accumulated weights for each flow, using the Dijkstra Algorithm. Then the flow uses this route for data transmission thereafter until the network topology information and node's load information change. When a new flow arrives, the PNC will re-schedule the transmission route for each flow as the network topology and traffic loads have changed.

The PNC then checks the concurrent transmission condition and schedules non-conflicting links to operate concurrently. During the random access period, PNC collects the network information and transmission requests, based on which PNC allocates network resources and distributes the scheduling information to nodes during the beacon period in one of the future superframes. It is possible that a node sends a transmission request to the PNC but does not receive the scheduling information within a certain time interval (e.g., a random access period plus a beacon period) because moving obstacles in the room may block the LOS link between the node and the PNC. In this case, the node needs to send its request in the next random access period. During the data transmission period, the PNC switches to the directional mode for data transmission. Nodes transmit data in the allocated time slots according to the scheduling information. If the data transmission is not successful due to blocked LOS by moving obstacles, the failure should be reported to the PNC during the next random access period so that the PNC can re-schedule the transmission in the next transmission period.

Next, we develop a scheduling algorithm for concurrent transmissions. For a given network topology, some hops in dense areas may have a lower probability to operate concurrently with other hops. Therefore, we should give higher priority of scheduling to the hops with less transmission opportunity but with heavy traffic loads. To achieve this, we sort hops in a descending order of transmission loads to guarantee that the hops with the highest loads will be scheduled first. The detailed algorithm is described as follows. Initially, there are L slots in a transmission period. A transmission request $r_{i,j}$ (i.e., the j-th hop of flow i) needs $n(i,j)$ slots. The PNC sequentially checks the hops to be scheduled in the descending order of their traffic loads and schedules non-conflicting links to operate concurrently according to the concurrent transmission condition: concurrent transmission is feasible if and only if any transmitter is outside the beamwidth of the other receiver or does not direct its beam to the other receiver if it is within the beamwidth of the other receiver. Two adjacent links which share one node cannot operate concurrently due to half-duplex operations of wireless transmission. If a link does not conflict with all existing hops in the group, this link is added in the group for concurrent transmissions and the PNC updates the reserved slots for this group based on the maximum number of required time slots of all the hops in the group. If a hop is not added in the current group, the PNC will sequentially check the following groups for concurrent transmissions. If a hop can not be added in any existing groups, the PNC will create a new group for this hop if the number of available slots in the superframe is sufficient. Otherwise, the PNC rejects the request due to limited network resources. In this case, the PNC will remove all hops involved in the flow where the rejected hop belongs to. The pseudo code for the concurrent transmission scheduling algorithm is shown in Algorithm 1.

Algorithm 1 Concurrent Transmission Scheduling Scheme

BEGIN:
1: PNC receives $r_{i,j}$ requesting $n(i,j)$ time slots
2: **for** All non-empty group $(T_b! = \text{Null})$ **do**
3:     **if** $r_{i,j}$'s link does not conflict with those of all existing links in T_b **then**
4:         **if** $r_{i,j}$ does not have shared nodes with other links in T_b **then**
5:             **if** $r_{i,j}$ requires extra slots, $n(i,j) - n(b) > 0$ **then**
6:                 **if** Available slots $L \geq n(i,j) - n(b)$ **then**
7:                     Schedule $r_{i,j}$ in group T_b;
8:                     Update $T_b = T_b \bigcup \{r_{i,j}\}$;
9:                     Update the available slots $L = L - [n(i,j) - n(b)]$;
10:                Update $n(b) = n(i,j)$;
11:                Update the allocated slots for $r_{i,j}$;
12:                Sort all hops in the decreasing order of loads.
13:                Go to END;
14:             **else**
15:                Go to line 26;
16:             **end if**
17:         **else**
18:             Schedule $r_{i,j}$ in T_b;
19:             Update $T_b = T_b \bigcup \{r_{i,j}\}$;
20:             Update the allocated slots for $r_{i,j}$;
21:             Sort all hops in the decreasing order of loads.
22:             Go to END;
23:         **end if**
24:         **end if**
25:     **end if**
26:     Next Group;
27: **end for**
28: **if** The number of available slots is larger than $n(i,j)$ **then**
29:     Start a new group $T(k) = \{r_{i,j}\}$;
30: **else**
31:     Reject request $r_{i,j}$ and release the reserved resources for all the hops in flow i;
32: **end if**
END;

IV. PERFORMANCE ANALYSIS

We use multi-hop transmissions to address the link outage problem and combat severe propagation loss at mmWave band to improve flow throughput. Concurrent transmissions are more favorable than serial TDMA transmissions in terms of network throughput [20], [24]. In this section, we analyze the performance of the proposed MHCT scheme on spatial reuse and time division multiplexing gain.

A. Spatial Multiplexing

To exploit the spatial multiplexing gain, communication links that do not interfere with each other can operate concurrently over the same mmWave channel. With short link length, the overlap area between the beamwidth of the transceivers and the area of WPAN is likely to be smaller in comparison to that with long link length. Therefore, there are probably more concurrent links in the whole area, according to the concurrent transmission condition. Hence, the channel can be utilized more efficiently by replacing a single long hop with multiple short hops using the relaying mechanism. In the following, we derive the average concurrent transmission probability as a function of link lengths, to show the spatial multiplexing gain achieved by the MHCT scheme.

Consider an indoor circle area S with radius R. As shown in Fig. 3, there are two pairs of transmitters and receivers randomly distributed in the circle area S. The transmitter and the receiver direct their beams to each other for data transmission. S_{R1} is the overlap area between S and the beamwidth of receiver R_1, while S_{T2} is the overlap area between S and the beamwidth of transmitter T_2. The probability that transmitter T_2 is outside the beamwidth of receiver R_1 is $1 - \frac{S_{R1}}{S}$. The probability that T_2 is located in the beamwidth of R_1 but does not direct its beam to R_1 is $\frac{S_{R1}}{S}(1 - \frac{S_{T2}}{S})$. Then the probability that transmitter T_2 does not interfere with receiver R_1 is

$$
\begin{aligned}
P &= (1 - \frac{S_{R1}}{S}) + \frac{S_{R1}}{S}(1 - \frac{S_{T2}}{S}) \\
&= 1 - \frac{S_{R1} \times S_{T2}}{S^2}
\end{aligned}
\tag{8}
$$

Similarly, the probability that transmitter T_1 does not interfere with receiver R_2 is $P' = 1 - \frac{S_{R2} \times S_{T1}}{S^2}$. Therefore, $Q = PP'$ is the probability that two links do not conflict with each other, thus they can operate concurrently.

A polar coordinate system O_1 is established with the center of circle area S as the origin. Then the position of transmitter T_1 is given by (r, α) in system O_1. Similarly, a polar coordinate system O_2 is built with transmitter T_1 as the origin and the position of the corresponding receiver R_1 is given by
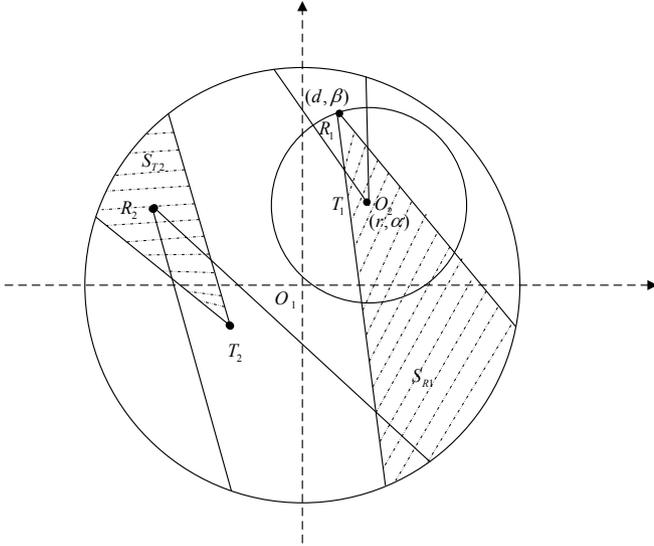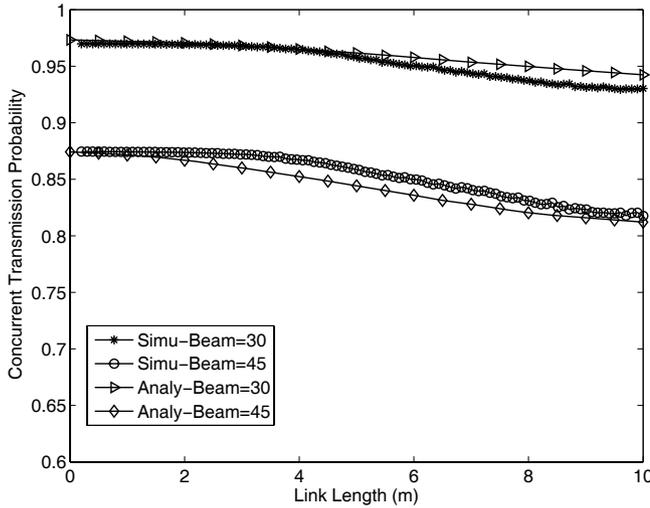
Fig. 3. Concurrent transmissions in WPANs.

Fig. 4. Probability Q versus link length.

(d, β) in the polar coordinate system O_2. d is the distance between transmitter T_1 and receiver R_1, i.e., link length. Due to symmetry, we only consider the case $0 \leq \alpha \leq \frac{\pi}{2}$. To make the analysis tractable, the overlapping area of S_{R1} is approximated as a triangle as follows,

$$\begin{cases} \frac{1}{2}g(a,b,\theta)g(a,b,-\theta), & -\frac{\pi}{2}+\frac{\theta}{2} < \beta < \frac{\pi}{2}-\frac{\theta}{2} \\ -\frac{1}{2}g(a,b,\theta)g(-a,-b,-\theta), & \frac{\pi}{2}-\frac{\theta}{2} < \beta < \frac{\pi}{2}+\frac{\theta}{2} \\ \frac{1}{2}g(-a,-b,\theta)g(-a,-b,-\theta), & \frac{\pi}{2}+\frac{\theta}{2} < \beta < \frac{3\pi}{2}-\frac{\theta}{2} \\ -\frac{1}{2}g(-a,-b,\theta)g(a,b,-\theta), & \frac{3\pi}{2}-\frac{\theta}{2} < \beta < \frac{3\pi}{2}+\frac{\theta}{2} \end{cases} \quad (9)$$

where $a = r\cos\alpha + d\cos\beta$, $b = r\sin\alpha + d\sin\beta$, θ is the antenna beamwidth, and the function $g(a, b, \theta)$ is defined as

$$g(a,b,\theta) = \cos(\beta - \frac{\theta}{2}) \mid \sqrt{\frac{R^2}{\cos^2(\beta-\frac{\theta}{2})} - [a\tan(\beta-\frac{\theta}{2})-b]^2} + a + b\tan(\beta-\frac{\theta}{2}) \mid \quad (10)$$

Substituting (10) into (9), S_{R1} becomes a function of r, α, d, β and θ, i.e., $S_{R1} = G(r, \alpha, d, \beta, \theta)$. To obtain the average probability $\overline{P}$, we have

$$\overline{P} = 1 - \frac{\overline{S_{R1}} \times \overline{S_{T2}}}{S^2}. \quad (11)$$

In the following, we derive $\overline{S_{R1}}$ and $\overline{S_{T2}}$ to obtain $\overline{P}$. Integrating $G(r, \alpha, d, \beta, \theta)$ with respect to β yields

$$G(r, \alpha, d, \theta) = \int_\beta f(\beta)G(r, \alpha, d, \beta, \theta)d\beta \quad (12)$$

where $f(\beta)$ is the probability density function of β. The receiver is uniformly distributed on the circle with d as the radius and the transmitter as the origin, or on part of the circle within the WPAN area if $R - r < d < R + r$, i.e., the two circles in Fig. 3 intersect each other. Therefore, the pdf of β is

$$f(\beta) = \begin{cases} \frac{1}{2\pi}, & (0 \leq \beta < 2\pi, \ 0 < d \leq R-r) \\ \frac{1}{\beta_2 - \beta_1}, & (\beta_1 \leq \beta \leq \beta_2, \ R-r < d < R+r) \\ 0, & (R+r \leq d) \end{cases} \quad (13)$$

where β_1 is determined by $\cos\beta_1 = \frac{(R^2-r^2-d^2)\cos\alpha - \sin\alpha\sqrt{4R^2r^2-(R^2+r^2-d^2)^2}}{2rd}$ and $\sin\beta_1 = \frac{(R^2-r^2-d^2)\sin\alpha + \cos\alpha\sqrt{4R^2r^2-(R^2+r^2-d^2)^2}}{2rd}$ while $\cos\beta_2 = \frac{(R^2-r^2-d^2)\cos\alpha + \sin\alpha\sqrt{4R^2r^2-(R^2+r^2-d^2)^2}}{2rd}$ and $\sin\beta_2 = \frac{(R^2-r^2-d^2)\sin\alpha - \cos\alpha\sqrt{4R^2r^2-(R^2+r^2-d^2)^2}}{2rd}$ give the value of β_2. Then, $\overline{S_{R1}}$ is given by

$$\begin{aligned} \overline{S_{R1}} &= G(d, \theta) \\ &= \int_0^R \int_0^{2\pi} f(r, \alpha)G(r, \alpha, d, \theta)d\alpha dr \\ &= 4\int_0^R \int_0^{\frac{\pi}{2}} f(r, \alpha)G(r, \alpha, d, \theta)d\alpha dr \quad (14) \end{aligned}$$

where $f(r, \alpha)$ is the joint pdf of r and α. The transmitter is uniformly distributed in the WPAN area, thus the joint probability density function of r and α is

$$f(r, \alpha) = \frac{r}{\pi R^2} \quad (0 \leq \alpha < 2\pi, \ 0 < r \leq R) \quad (15)$$

Similarly, we can also obtain $\overline{S_{T2}}$ as a function of link length d' between R_2 and T_2. Therefore, the average probability $\overline{P}$ is a function of the link length d and d'. Following the same procedure, we can also obtain $\overline{P'}$ as a function of link length d' and d. The average probability that two links can operate concurrently ($\overline{Q} = \overline{PP'}$) is a function of the link lengths of the two links. This function indicates how the spatial multiplexing gain varies with link lengths on average. Fig. 4 shows the numerical results of the average probability $\overline{Q}$ that concurrent transmission in two communication links can
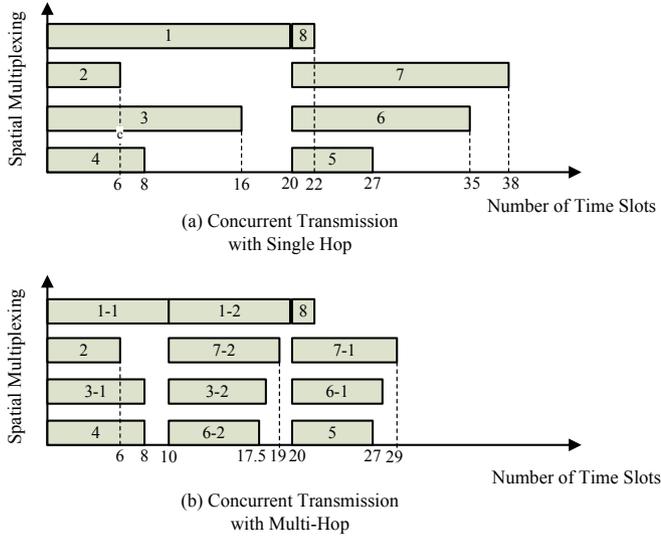
Fig. 5.   Illustration for time division multiplexing

Fig. 6.   Probability density function of required number of time slots.

take place as a function of the link lengths with different antenna beamwidths (to simply show the numerical results, let $d = d'$). The probability $\overline{Q}$ decreases as the link length becomes larger. Therefore, the proposed MHCT scheme can exploit more spatial reuse, i.e., it can support more concurrent links in mmWave WPANs.

B. Time Division Multiplexing

According to (3), the data transmission rate is a function of the link length. Thus, data transmissions over each link may require a different number of time slots. In Fig. 5 (a), a schedule is shown for the SHCT scheme. The required number of time slots of links 2, 4, 5 and 8 are far fewer than the number of time slots reserved for the groups they are scheduled in. It can be expected to utilize the resource more efficiently by properly breaking the single long hop into multiple short hops. For example, as shown in Fig. 5 (b), by breaking a long hop (i.e., hops 1, 3, 6 and 7) into two short hops, the total number of time slots for eight flows is reduced from 38 to 29 although the number of groups increases from 2 to 3. Replacing single long hops with multiple short hops can save transmission time, thus the flow throughput and network throughput are enhanced greatly.

To make the performance of single hop concurrent transmission and multi-hop concurrent transmission schemes comparable with time division multiplexing, we consider that the average number of concurrent links for each transmission group in the MHCT scheme is the same as that in the SHCT scheme. N flows are divided into N' ($N' > N$) links for multi-hop transmissions. To make the analysis tractable, we study a conservative case that there are no concurrent transmissions for intra-flow links. In this case, all the links in the same group are independent. WPANs usually cover a limited area and only a few links are involved in each flow. The limited number of hops for each flow and the half-duplex transmission make the intra-flow links difficult to operate concurrently.

Let X denote the number of reserved slots for a group, which is defined as the maximum number of required time
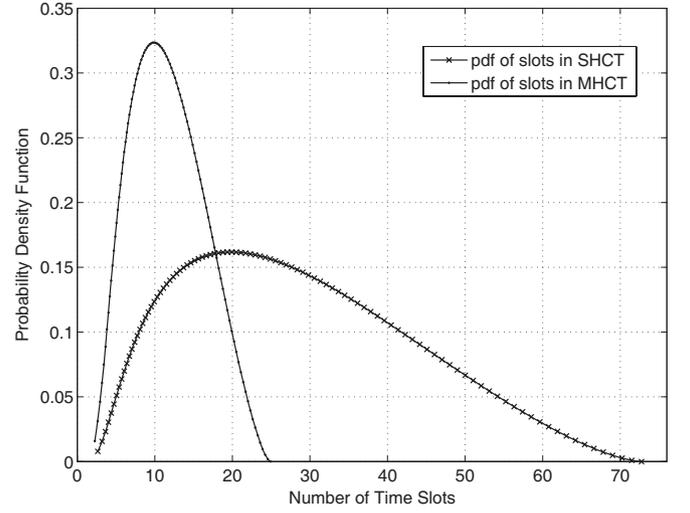
slots among all the links in the group. The cumulative distribution function (cdf) of X is given by

$$
\begin{aligned}
F_X(x) &= P(X \le x) \\
&= P(X_1 \le x, X_2 \le x \ldots X_M \le x) \quad (16)
\end{aligned}
$$

where X_m ($m = 1, 2 \ldots M$) is the number of slots requested by the mth link in the group. The X_m's are i.i.d. random variables with pdf $\widetilde{f}(x)$ for the SHCT scheme and pdf $\overline{f}(x)$ for the MHCT scheme. Therefore, we have

$$
F_X(x) = \prod_{m=1}^{M} P(X_m \le x) = [\widetilde{F}(x)]^M \quad (17)
$$

where $\widetilde{F}(x) = \int_0^x \widetilde{f}(x)dx$. The pdf of X is thus given by

$$
f_X(x) = \frac{dF_X(x)}{dx} = M\widetilde{f}(x)[\widetilde{F}(x)]^{M-1} \quad (18)
$$

The expected number of time slots reserved for each group is

$$
\begin{aligned}
E[X] &= \int_{x_a}^{x_b} x f_X(x) dx \\
&= \int_{x_a}^{x_b} x M \widetilde{f}(x)[\widetilde{F}(x)]^{M-1} dx \quad (19)
\end{aligned}
$$

where x_a and x_b are respectively the minimum and maximum required numbers of slots among all the hops in a group. Then we have $\widetilde{F}(x_a) = 0$ and $\widetilde{F}(x_b) = 1$. The total required number of slots for N flows using the SHCT scheme is

$$
T_{SHCT} = \frac{N}{M}E[X] = N \int_{x_a}^{x_b} x[\widetilde{F}(x)]^{M-1}\widetilde{f}(x)dx \quad (20)
$$

Similarly, the total number of time slots for N flows using the MHCT scheme is given by

$$
T_{MHCT} = N' \int_{x_a'}^{x_b'} x[\overline{F}(x)]^{M-1}\overline{f}(x)dx \quad (21)
$$

where $\overline{F}(x) = \int_0^x \overline{f}(x)dx$.

In (21), the total number of time slots for N flows with the MHCT scheme depends on the number of hops, the average number of concurrent transmissions, and the required
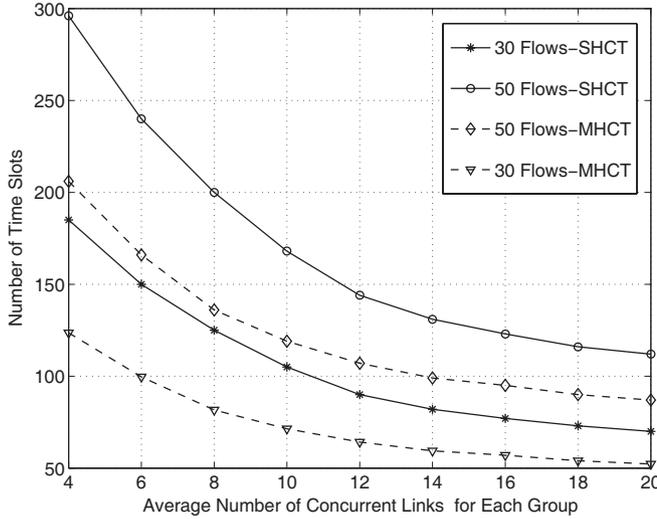
Fig. 7.   Time division multiplexing

TABLE I
SIMULATION PARAMETERS

Parameters	Symbol	Value
System bandwidth	W	1200 MHz
Transmission power	P_T	0.1mW
Background noise	N_0	-134dBm/MHz
Path loss exponent	n	2
Reference distance	d_{ref}	1.5m
Path loss at d_{ref}	PL_0	71.5 dB
Slot time	ΔT	$18\mu s$
Beacon period	T_{bea}	50 μs
Random access period	T_{ran}	800 μs
Number of slots in transmission period	$\overline{N}$	1000
Probability of NLOS link	p	0.1
NLOS period for each link	T_{NLOS}	0.2ms

number of time slots for each hop. Therefore, the hop selection metric plays a crucial role in achieving the time division multiplexing gain in the MHCT scheme. In [31], the pdf of the distance between two nodes randomly picked in a circle area with radius R is $f(d) = \frac{4d}{\pi R^2}cos^{-1}(\frac{d}{2R}) - \frac{2d^2}{\pi R^3}\sqrt{1 - \frac{d^2}{4R^2}}$. The pdf of link length in the MHCT scheme is obtained by shrinking the pdf of link length in SHCT by a half, $f(d) = \frac{16d}{\pi R^2}cos^{-1}(\frac{d}{R}) - \frac{16d^2}{\pi R^3}\sqrt{1 - \frac{d^2}{R^2}}$. Without loss of generality, we choose $N' = 2N$ to show the numerical results. The transmission rate is calculated according to (3). With the same traffic demands for each flow, we can get $\overline{f}(x)$ and $\widehat{f}(x)$ numerically as shown in Fig. 6. The required numbers of time slots for various number of traffic flows with the MHCT scheme and the SHCT scheme are shown in Fig. 7. We can see that the proposed multi-hop concurrent transmission scheme greatly improves the time division multiplexing gain. With the MHCT scheme, it takes less time to transmit the same number of traffic flows, thus the network throughout and flow throughput are enhanced.

C. Per-Flow Throughput

In this subsection, we analyze the per-flow throughput for a given schedule, which specifies a set of links that are active in each time slot. The per-flow throughput is defined as the ratio of the transmitted data of the flow to the time duration assigned to the flow in a superframe. In the proposed concurrent transmission scheduling scheme, a transmission request $r(i,j)$ requires $n(i,j)$ slots while the allocated number of slots is larger than or equal to $n(i,j)$ by taking the advantage of concurrent transmissions in all links in a group. Let T_y denote the number of time slots allocated for the yth group (G_y) in a valid schedule. If $r(i,j)$ is successfully scheduled in the yth group,

$$T(i,j) = T_y \qquad (22)$$

where $T(i,j)$ is the number of time slots assigned to the jth hop of flow i. The throughput of flow i is

$$F_i = \frac{C(i,j)n(i,j)}{\sum_{y=1}^{Y} T_y I_{i,y}} \qquad (23)$$

where $C(i,j)$ is the channel capacity of hop j of flow i, Y is the total number of groups, and $I_{i,y}$ is the identification function defined as

$$I_{i,y} = \begin{cases} 1, & \text{for } \forall j, n(i,j) \in G_y \\ 0, & \text{otherwise.} \end{cases} \qquad (24)$$

V. PERFORMANCE EVALUATION

In this section, we describe the performance evaluation methodology and present the simulation results for the proposed MHCT scheme compared with the traditional single hop transmission schemes.

We evaluate the performance of the proposed scheme in terms of average flow throughput, network throughput, resource utilization efficiency, and energy consumption in a typical mmWave WPAN environment (i.e., large office space), using a simulator coded in C++. The PNC is placed in the center of the room and 40 wireless nodes are randomly distributed in the room, which is a circle area with the radius of 8 meters. Each node is equipped with a directional antenna with a beamwidth of $60°$, corresponding to six beams at each node. A node can communicate with all the other nodes within its transmission range if the LOS link is available. Obstacles may block the LOS link between the source and the destination with probability p and for a duration of T_{NLOS}. The path loss at the reference distance, d_{ref}, is denoted as PL_0. We set up various numbers of flows with constant bit rates and randomly select the source and destination nodes for each flow. The holding time of each flow is uniformly distributed with a variable mean between 0.5 minute and 2 minutes. The main parameters used in our simulations are listed in Table I.

We compare the proposed MHCT scheme with two other transmission schemes, namely, SHCT [20] and single hop transmission (SHT). In the SHCT scheme, if LOS link is unavailable, a neighboring WN is randomly selected to relay the traffic [19]. We use the SHT scheme operating in a TDMA mode as the baseline for comparison.

Fig. 8 shows the average flow throughput versus various numbers of traffic flows in the network. The average flow throughput decreases if more flows in the WPAN are competing for the network resource. The MHCT scheme outperforms the SHCT scheme on flow throughput due to the path selected
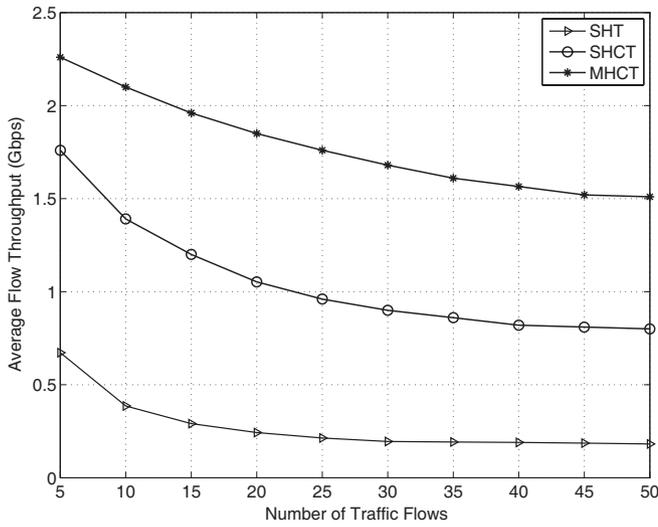
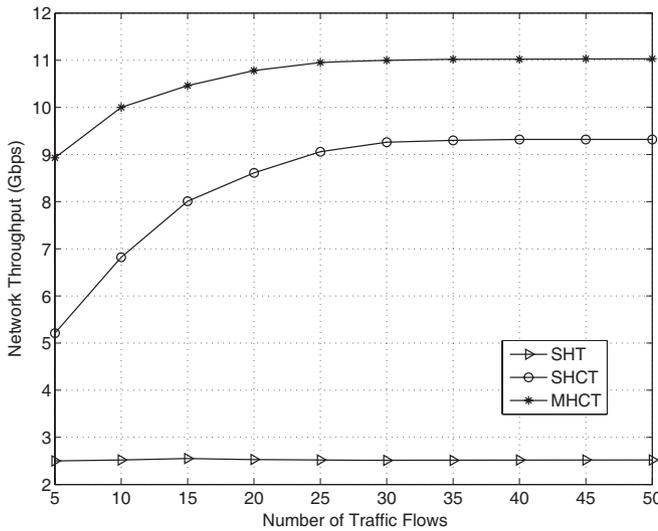Fig. 8. Average flow throughput versus the number of traffic flows.

Fig. 9. Network throughput versus the number of traffic flows.

Fig. 10. Time resource utilization efficiency versus the number of traffic flows.

Fig. 11. Energy consumption per Gigabit.

according to (7) and more efficient time multiplexing. In addition, with concurrent transmission more flows share the time slots; therefore each flow might be allocated with more time slots. Hence the long-term throughput of each flow will be improved.

The network throughput of the three schemes is shown in Fig. 9. In the SHT scheme, there is at most one transmission at any time in the network. Concurrent transmissions can improve the spatial reuse and significantly increase the network throughput. It is also shown that the proposed MHCT scheme achieves higher network throughput compared with the SHCT scheme because, with the MHCT scheme, the number of concurrent links is larger and the transmission rate of each link is higher due to the short link length.

Fig. 10 shows the time utilization efficiency, which is defined as the average number of active links in each time slot during the data transmission period. The time resource utilization efficiency for the SHT scheme is 1 because it does not support concurrent transmissions. The MHCT scheme outperforms the SHCT scheme on time resource utilization
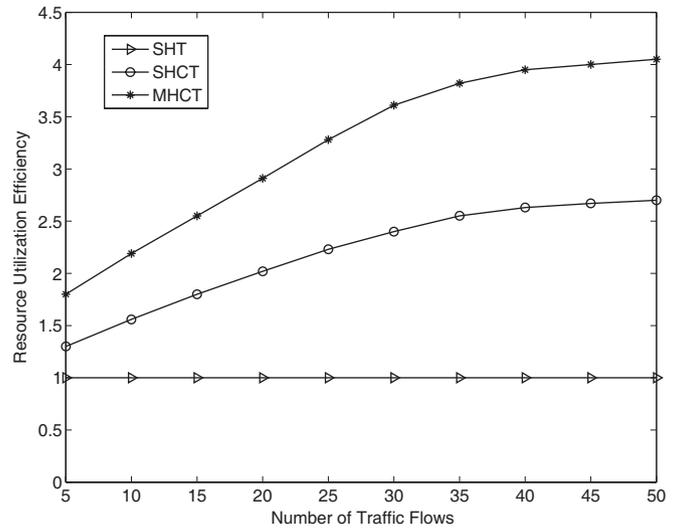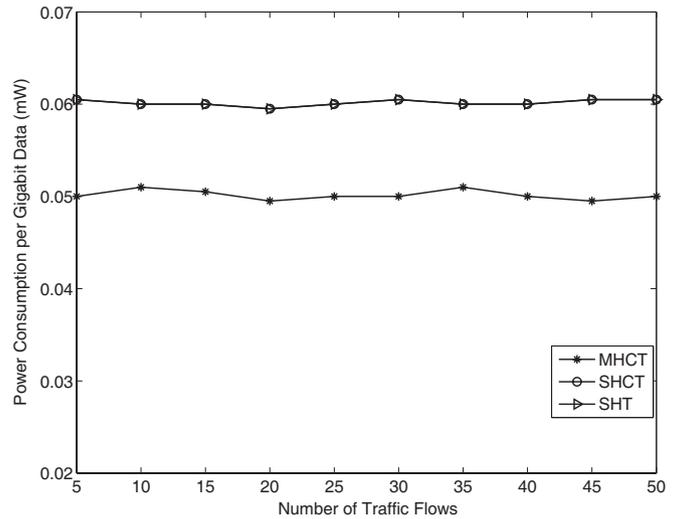
efficiency because it achieves higher spatial reuse and time division multiplexing gain.

We then compare the energy consumption of the proposed scheme with that of SHT and SHCT. For fair comparison, we divide the sum transmission power used by all flows during a superframe by the total amount of transmitted data, to obtain the power consumption per Gbits. From Fig. 11, we can see that our proposed scheme is more energy efficient than SHT and SHCT. This is because, by properly breaking a single long hop into multiple shorter hops, the total number of required slots can be reduced and the flow throughput can be improved accordingly. Therefore, the allocated time to each flow can be greatly reduced, which results in a lower energy consumption. Although SHCT achieves a higher network throughput than SHT, the energy consumption of each flow does not change, and thus SHCT and SHT achieves the same performance in terms of energy consumption per Gbits.

VI. RELATED WORK

A wide range of protocols and algorithms for wireless networks have been proposed for transmission scheduling [17], [18], [20], [22], [28]. One line of research uses graph representation of wireless networks to model the interference or SINR at the receiver [17], [18], [28]. The accumulated interference among concurrent transmissions is taken into account to make the signal decoding successful with acceptable SINR. On the other hand, the transmissions which do not cause significant interference to each other can be scheduled for concurrent transmissions [20], [22]. It is shown that concurrent transmissions can improve the network throughput significantly if the co-channel interference is properly managed.

Several work on mmWave WPANs using directional antenna has appeared in the literature [8], [19]–[21], [23], [24]. Cross-layer modeling and design approaches are presented in [19] for mmWave WPANs to account for the problems of directionality and blockage. It uses minimum number of hops for data transmission. Specifically, if the LOS link is available between the source and the destination, single hop transmission is employed; otherwise, an intermediate node is randomly selected as the relay. In [20], an exclusive region (ER) based resource management scheme is proposed to exploit the spatial reuse of mmWave WPANs with directional antenna and the optimal ER sizes are analytically derived in [21]. In [24], the Virtual Time-slot Allocation (VTSA) scheme is designed to allow the TDMA time slots to be reused by multiple communication links simultaneously to increase the system throughput and, at the same time, the VTSA scheme monitors the potential performance degradation due to co-channel interference. In [8], the throughput of mmWave system is analyzed, based on a hybrid multiple access of CSMA/CA and TDMA. It also evaluates a method for optimizing the throughput of the system by reducing the collisions in the CSMA/CA time-slots using a private channel release time. To the best of our knowledge, the previous work in mmWave WPAN uses single hop for data transmission or one relay if LOS link is unavailable. Taking into account the unique features of mmWave WPANs (such as LOS transmission, short transmission range, and high propagation loss), it is very likely that deploying multi-hop transmissions in mmWave WPANs can improve the flow throughput. With concurrent transmissions, our proposed scheme can further improve the network throughput.

VII. CONCLUSION

In this paper, we have proposed a multi-hop concurrent transmission scheme for mmWave WPANs. Taking the unique characteristics of mmWave WPANs (i.e., high propagation loss, LOS link and directional antenna) into consideration, the proposed MHCT scheme exploits the spatial reuse and time division multiplexing gain, thus significantly improves the network throughput and flow throughput compared with single hop transmission schemes. By replacing a single long hop with multiple short hops, the MHCT scheme can allow more communication links for concurrent transmissions. With the MHCT scheme, the mmWave WPANs can support higher

data rates to enable numerous multimedia applications requiring large bandwidth. The results should provide important guidelines for future research of mmWave WPANs, such as enabling multi-hop transmissions with efficient power control to further improve the resource utilization efficiency.

REFERENCES

[1] T. Manabe, Y. Miura, and T. Ihara, "Effects of antenna directivity and polarization on indoor multipath propagation characteristics at 60 GHz," *IEEE J. Sel. Areas Commun.*, vol. 14, no. 3, pp. 441–448, 1996.

[2] P. Smulders, "Exploiting the 60 GHz band for local wireless multimedia access: prospects and future directions," *IEEE Commun. Mag.*, vol. 40, no. 1, pp. 140–147, Jan. 2002.

[3] S. Singh, R. Mudumbai, and U. Madhow, "Distributed coordination with deaf neighbors: efficient medium access for 60 GHz mesh networks," in *Proc. IEEE INFOCOM*, Apr. 2010, pp. 1–9.

[4] N. Guo, R. C. Qiu, S. S. Mo, and K. Takahashi, "60-GHz millimeter-wave radio: principle, technology, and new results," *EURASIP J. Wireless Commun. and Networking*, ID 68253, 8 pages, Sep. 2006.

[5] R. Daniels and R. Heath, "60 GHz wireless communications: emerging requirements and design recommendations," *IEEE Veh. Technol. Mag.*, vol. 2, no. 3, pp. 41–50, Sep. 2007.

[6] J. Foerster, J. Lansford, J. Laskar, T. S. Rappaport, and S. Kato, "Realizing Gbps wireless personal area networks," *IEEE J. Sel. Areas Commun.*, vol. 27, no. 8, pp. 1313–1317, Oct. 2009

[7] J. Qiao, L. X. Cai, and X. Shen, "Multi-hop concurrent transmission in millimeter wave WPANs with directional antenna," in *Proc. IEEE ICC'10*, May 2010, pp. 1–5.

[8] C. W. Pyo and H. Harada, "Throughput analysis and improvements of hybrid multiple access in IEEE 802.15.3c mmWave-WPAN," *IEEE J. Sel. Areas Commun.*, vol. 27, no. 8, pp. 1414–1424, Oct. 2009

[9] (2009) Multi-Gb/s 60GHz Wireless Transceiver Design for Mobile Applications at Berkeley Wireless Research Center. Avaiable: http://bwrc.eecs.berkeley.edu/Research/ e-eis/60ghz_trans.html

[10] (2009) IBM's 60-GHz Page. Available: http://domino.watson.ibm.com/comm/research_projects.nsf/pages/mmwave.pubs.html.

[11] IEEE 802.15 WPAN Millimeter Wave Alternative PHY Task Group 3c (TG3c). Available: http://www.ieee802. org/15/pub/TG3c.html.

[12] IEEE 802.11 VHT Study Group. Available: http://www.ieee802.org/11/Reports/vht_update.htm.

[13] B. Radunovic and J. Le Boudec, "Optimal power control, scheduling, and routing in UWB networks," *IEEE J. Sel. Areas Commun.*, vol. 22, no. 7, pp. 1252–1270, Sep. 2004

[14] N. Deparis, C. Loyez, N. Rolland, and P. A. Rolland, "UWB in millimeter wave band with pulsed ILO," *IEEE Trans. Circuits and Systems*, vol. 55, no. 4, pp. 339–343, Apr. 2008

[15] F. Winkler, E. Fischer, E. Grass, and P. Langendörfer, "An indoor localization system based on DTDOA for different wireless LAN systems," in *Proc. WPNC06*, pp. 117–122.

[16] F. Gutierrez, S. Agarwal, K. Parrish, and T. S. Rappaport, "On-chip integrated antenna structures in CMOS for 60 GHz WPAN systems," *IEEE J. Sel. Areas Commun.*, vol. 27, no. 8, pp. 1367–1378, Oct. 2009

[17] T. Moscibroda, Y. A. Oswald, and R. Wattenhofer, "How optimal are wireless scheduling protocols?" in *Proc. IEEE INFOCOM'07*, May 2007, pp. 1433–1441.

[18] P. Dutta, V. Mhatre, D. Panigrahi, and R. Rastogi, "Joint routing and scheduling in multi-hop wireless networks with directional antennas," in *Proc. IEEE INFOCOM'10*, Mar. 2010, pp. 1–5.

[19] S. Singh, F. Ziliotto, U. Madhow, E. M. Belding, and M. J. W. Rodwell, "Millimeter wave WPAN: cross-layer modeling and multihop architecture," in *Proc. IEEE INFOCOM'07*, May 2007, pp. 2336–2240.

[20] L. X. Cai, L. Cai, X. Shen, and J. W. Mark, "REX: a Randomized EXclusive region based scheduling scheme for mmWave WPANs with directional antenna," *IEEE Trans. Wireless Commun.*, vol. 9, no. 1, pp. 113–121, Jan. 2010.

[21] L. X. Cai, L. Cai, X. Shen, and J.W. Mark, "Capacity analysis of UWB networks in three-dimensional space," *IEEE/KICS J. Commun. and Networks*, vol. 11, no. 3, pp. 287–296, 2009.

[22] Z. Yang, L. Cai, and W. Lu, "Practical concurrent transmission scheduling algorithms for rate-adaptive wireless networks," in *Proc. IEEE INFOCOM'10*, Mar. 2010, pp. 1–9.

[23] J. Wang, R. Venkatesha Prasad, and I. G. M. M. Niemegeers, "Enabling multi-hop on mm Wave WPANs," in *Proc. IEEE ISWCS'08*, Oct. 2008, pp. 371–375.

[24] C. Sum, Z. Lan, R. Funada, J. Wang, T. Baykas, M. A. Rahman, and H. Harada, "Virtual time-slot allocation scheme for throughput enhancement in a millimeter-wave multi-Gbps WPAN system," *IEEE J. Sel. Areas Commun.*, vol. 27, no. 8, pp. 1379–1389, Oct. 2009

[25] S. Y. Geng, J. Kivinen, X. W. Zhao, and P. Vainikainen, "Millimeter-wave propagation channel characterization for short-range wireless communications," *IEEE Trans. Veh. Technol.*, vol. 58, no.1, pp. 3–13, Jan. 2009

[26] R. Mudumbai, S. Singh, and U. Madhow, "Medium access control for 60 GHz outdoor mesh networks with highly directional links," in *Proc. IEEE INFOCOM'09*, Apr. 2009, pp. 2871–2875.

[27] R. R. Choudhury and N. Vaidya, "Performance of ad hoc routing using directional antennas," *Elsevier Ad Hoc Networks*, vol. 3, no. 2, pp. 157–173, Mar. 2005.

[28] A. Behzad and I. Rubin, "On the performance of graph-based scheduling algorithms for packet radio networks," in *Proc. IEEE GLOBECOM'03*.

[29] J. Zander, "Performance of optimum transmitter power control in cellular radio systems," *IEEE Trans. Veh. Technol.*, vol. 41, pp. 69–78, 1992.

[30] L. X. Cai, L. Cai, X. Shen, and J. W. Mark, "Resource management and QoS provisioning for IPTV over mmWave-based WPANs with directional antenna," *ACM Mobile Networks and Applications*, vol. 14, no. 2, pp. 210–219, 2009.

[31] http://mathworld.wolfram.com/DiskLinePicking.html

Jian Qiao received B.E. degree in Beijing University of Posts and Telecommunications, China in 2006 and the MASc degree in Electrical and Computer Engineering from University of Waterloo, Canada in 2010. He is currently working toward his PhD degree at the Department of Electrical and Computer Engineering, University of Waterloo, Canada. His research interests include millimeter wave WPANs, medium access control, resource management, and smart grid networks.

Lin X. Cai received her M.A.Sc. and PhD degrees in electrical and computer engineering from the University of Waterloo, Ontario, Canada, in 2005 and 2009, respectively. She is currently working as a postdoctoral research fellow at Princeton University. Her research interests include green communication and networking, resource management for broadband multimedia networks, and cross-layer optimization and QoS provisioning.

Xuemin(Sherman) Shen (F) received the B.Sc. (1982) degree from Dalian Maritime University (China) and the M.Sc. (1987) and Ph.D. degrees (1990) from Rutgers University, New Jersey (USA), all in electrical engineering. He is a Professor and University Research Chair, Department of Electrical and Computer Engineering, University of Waterloo, Canada. Dr. Shen's research focuses on resource management in interconnected wireless/wired networks, UWB wireless communications networks, wireless network security, wireless body area networks and vehicular ad hoc and sensor networks. He is a co-author of three books, and has published more than 500 papers and book chapters in wireless communications and networks, control and filtering. Dr. Shen served as the Technical Program Committee Chair for IEEE VTC'10, the Symposia Chair for IEEE ICC'10, the Tutorial Chair for IEEE ICC'08, the Technical Program Committee Chair for IEEE Globecom'07, the General Co-Chair for Chinacom'07 and QShine'06, the Founding Chair for IEEE Communications Society Technical Committee on P2P Communications and Networking. He also served as a Founding Area Editor for IEEE TRANSACTIONS ON WIRELESS COMMUNICATIONS; Editor-in-Chief for *Peer-to-Peer Networking and Application*; Associate Editor for IEEE TRANSACTIONS ON VEHICULAR TECHNOLOGY; *Computer Networks*; and *ACM/Wireless Networks*, etc., and the Guest Editor for IEEE JSAC, *IEEE Wireless Communications*, *IEEE Communications Magazine*, and *ACM Mobile Networks and Applications*, etc. Dr. Shen received the Excellent Graduate Supervision Award in 2006, and the Outstanding Performance Award in 2004 and 2008 from the University of Waterloo, the Premier's Research Excellence Award (PREA) in 2003 from the Province of Ontario, Canada, and the Distinguished Performance Award in 2002 and 2007 from the Faculty of Engineering, University of Waterloo. Dr. Shen is a registered Professional Engineer of Ontario, Canada, an IEEE Fellow, an Engineering Institute of Canada fellow, and a Distinguished Lecturer of IEEE Vehicular Technology Society and Communications Society.

Jon W. Mark (LF) received the Ph.D. degree in electrical engineering from McMaster University in 1970. In September 1970 he joined the Department of Electrical and Computer Engineering, University of Waterloo, Waterloo, Ontario, where he is currently a Distinguished Professor Emeritus. He served as the Department Chairman during the period July 1984-June 1990. In 1996 he established the Center for Wireless Communications (CWC) at the University of Waterloo and is currently serving as its founding Director. Dr. Mark had been on sabbatical leave at the following places: IBM Thomas J. Watson Research Center, Yorktown Heights, NY, as a Visiting Research Scientist (1976-77); AT&T Bell Laboratories, Murray Hill, NJ, as a Resident Consultant (1982-83): Laboratoire MASI, UniversitPierre et Marie Curie, Paris France, as an Invited Professor (1990-91); and Department of Electrical Engineering, National University of Singapore, as a Visiting Professor (1994-95).

He has previously worked in the areas of adaptive equalization, image and video coding, spread spectrum communications, computer communication networks, ATM switch design and traffic management. His current research interests are in broadband wireless communications, resource and mobility management, and cross domain interworking.

A Life Fellow of IEEE and a Fellow of the Canadian Academy of Engineering, Dr. Mark is the recipient of the 2000 Canadian Award for Telecommunications Research and the 2000 Award of Merit of the Education Foundation of the Federation of Chinese Canadian Professionals. He was an editor of IEEE TRANSACTIONS ON COMMUNICATIONS (1983-1990), a member of the Inter-Society Steering Committee of the IEEE/ACM TRANSACTIONS ON NETWORKING (1992-2003), a member of the IEEE Communications Society Awards Committee (1995-1998), an editor of *Wireless Networks* (1993-2004), and an associate editor of *Telecommunication Systems* (1994-2004).